

Magnetic behavior in Mg-stabilized bcc β -Gd and β -Dy

J. W. Herchenroeder* and K. A. Gschneidner, Jr.

Ames Laboratory and Department of Materials Science and Engineering, Iowa State University, Ames, Iowa 50011

(Received 26 September 1988; revised manuscript received 23 January 1989)

bcc β -Gd and β -Dy, stabilized by Mg additions, exhibit spin-glass-like behavior. Both systems show field-cooling effects in the magnetic susceptibility which is indicative of spin freezing reactions. The β -Gd alloys order ferromagnetically (< 80 K) first on cooling before undergoing a Gabay-Toulouse-type reentrant spin-glass transition (< 50 K) into a mixed ferromagnetic plus spin-glass phase. Low-field ac susceptibility measurements show both the Curie and spin freezing transitions. Low-temperature heat capacity (down to 1.5 K) shows evidence of both ferromagnetic and spin-glass excitations. A magnetic phase diagram predicts a pure spin-glass phase for Gd concentrations up to 66 at. % Gd. The β -Dy alloys exhibit a cusp in the ac susceptibility characteristic of spin-glass behavior. Field-cooled magnetic-susceptibility measurements suggest a close competition between antiferromagnetism and spin-glass behavior. The occurrence of the maximum in the magnetic susceptibility at 1.4 T is evidence that some atoms may order antiferromagnetically. A large linear heat-capacity term which is probably due to both the electronic specific heat γ and a spin-glass contribution plus the presence of large T^2 and T^3 terms support the mixed-state hypothesis. The metastable bcc Gd-Mg and Dy-Mg alloys are unique in that they have the highest concentration of magnetic atoms in a *crystalline, metallic* spin glass (> 70 at. % Gd or Dy).

I. INTRODUCTION

Over 20 years ago, when the high-temperature allotropy of the rare-earth metals was being first investigated, it was shown¹ that a high-temperature bcc phase of the heavy rare-earth metals could be retained at room temperature by alloying with Mg and ice-water quenching. This relatively simple procedure affords an excellent opportunity to directly compare the physical properties of a rare-earth element in two different crystal structures—the bcc phase and the room-temperature close-packed structure (fcc, hcp, or dhcp)—by extrapolating the physical property of the metastable bcc alloys to a theoretical pure bcc material. A systematic study² carried out on La alloys showed that only Cd is as effective as Mg in stabilizing the bcc structure. Comparison of the superconducting transition temperature of the three La allotropes (dhcp, fcc, and bcc) has been done³ using this method.

For the magnetic lanthanides such as Gd and Dy, the bcc structure offers a more symmetric crystal field than is found in the equilibrium hcp room-temperature phase. In pure metals, the hexagonal crystal field strongly influences the type of magnetic ordering, so one might expect different types of ordering and different temperatures for a bcc structure. Gd has no orbital magnetic moment ($L=0$) in its normal state, and therefore will have only minimal crystal-field interactions in either the hcp or bcc structure. Any difference in the magnetic properties of the two phases is limited to atomic spacing or magnetic dilution by Mg for the bcc phase. Dy was chosen as the companion system because it has both anti-

ferromagnetic and ferromagnetic transitions for the pure metal. The results of our study are described below.

II. EXPERIMENTAL PROCEDURES

A. Alloy preparation

The rare-earth Mg systems form eutectoid phase diagrams as in the Gd-Mg phase diagram (Fig. 1). The Dy-Mg phase diagram is not known, but it should be similar to the Gd-Mg system.⁴ For both Gd and Dy the room-temperature allotrope α is hcp. On heating, there is a transformation to bcc β before melting.

The proper proportions of the lanthanide and Mg were sealed together in a Ta capsule under a He partial pressure. The Mg was sublimed from commercial stock and was 99.998 at. % pure. The rare-earth metals were produced at the Ames Laboratory Materials Preparation Center. The total transition-metal impurity content was less than 30 ppm atomic. The total rare-earth impurity was less than 10 ppm atomic. The total interstitial impurities, e.g., O, N, and H ranged up to 1000 ppm atomic.

Each alloy was melted and inverted several times in an induction furnace to insure homogeneity. For quenching the alloy was remelted in a resistance furnace and quenched in ice water from at least 25 °C above the melting point. On cooling the bcc phase forms from the liquid, which is subsequently frozen in as the quench accelerates through the eutectoid temperature. Single-phase bcc alloys could be stabilized easiest at the eutectoid composition. Stabilization becomes more difficult as

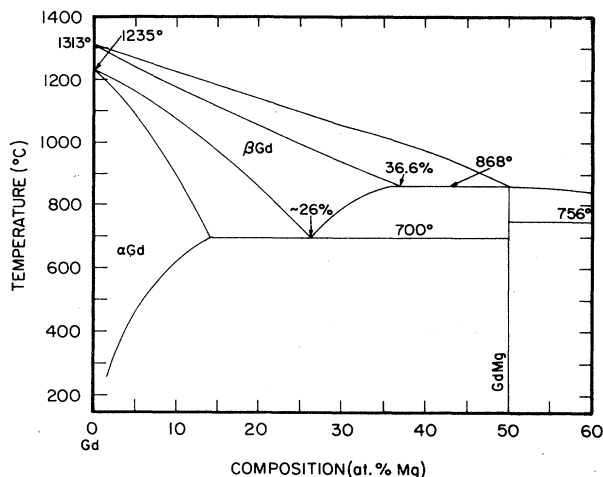


FIG. 1. The Gd-Mg system (Ref. 4).

the composition is moved away from the eutectoid composition with the result being a composition window about 5% wide where the bcc phase can be stabilized. Metallographic examination shows a dendritic microstructure from the initial freezing which raises the possibility of concentration gradients. X-ray-diffraction patterns show sharp reflections with no evidence of a second phase. A complete discussion of the metallurgical aspects of these nonequilibrium alloys will be reported in another paper.

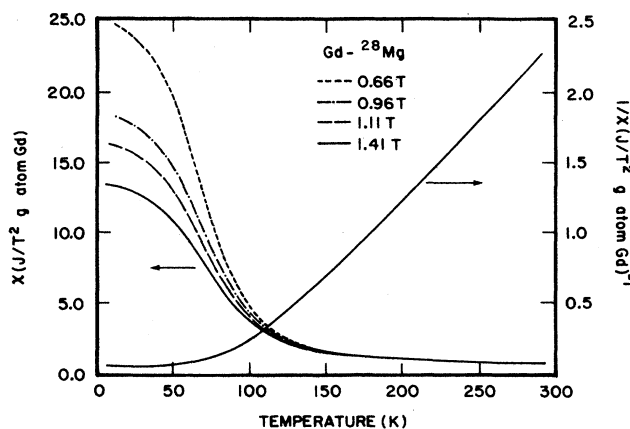
B. Apparati

Magnetic susceptibility was measured on three different devices. High-field (0.5 to 1.8 T) measurements were made using a Faraday balance calibrated by the National Bureau of Standards (NBS) Pt and Pd standards. Low-field measurements (0.005 to 0.2 T) were made in a SQUID magnetometer. The SQUID measures a volume susceptibility while the Faraday method measures a gram susceptibility. The density conversion factor was determined by comparison of paramagnetic susceptibilities from each method. All the values are reported in units per gram of lanthanide. Finally ac susceptibility was measured at extremely low field (2.5×10^{-6} T) at 100 Hz. The units are arbitrary, but the values are normalized with respect to the lanthanide content. The heat capacity was measured from 1.3 to 60 K in a semiadiabatic pulse calorimeter.

III. EXPERIMENTAL RESULTS

A. β -Gd

An alloy containing 28 at. % Mg is representative of the other alloys and its susceptibility χ per gram Gd (i.e., per mole of Gd) is shown in Fig. 2 for measuring fields greater than 0.5 T. Above 120 K the alloy is paramagnetic. On cooling the alloy orders into a weak ferromagnetic state.

FIG. 2. Magnetic susceptibility for the Gd-²⁸Mg alloy, which is typical of all the Gd alloys.

Above 120 K the β -Gd alloys behave as normal paramagnets. A plot of the inverse susceptibility (Fig. 2) for the alloys is linear above T_c following the Curie-Weiss law. χ^{-1} is independent of the applied field suggesting minimal ferromagnetic impurities (i.e., α -Gd). The effective paramagnetic moment per Gd atom, p_{eff} , is calculated from the slope, and the temperature intercept gives Θ_p , the paramagnetic Curie temperature. Θ_p decreases with increased Mg content due to the increased amount of magnetic dilution. These values are summarized for the β -Gd alloys in Table I.

The alloys order in what appears to be a ferromagnetic state at T_c some 20–30 K less than the value of Θ_p . The

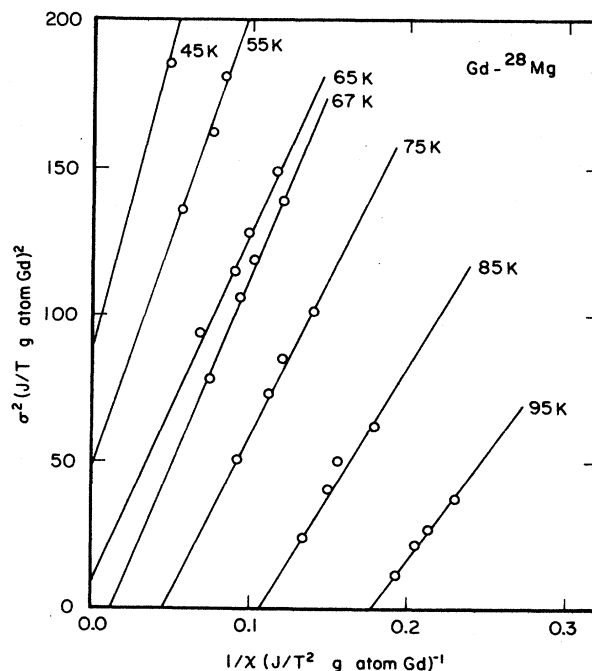
FIG. 3. Arrott plot for Gd-²⁸Mg. $T_c = 66$ K.

TABLE I. Summary of magnetic behavior in β -Gd.

Alloy	C	P_{eff}	Θ_p	T_c	T_f
	$\left[\frac{\text{JK}}{T^2 \text{ g atom Gd}} \right]$				
Gd- ²³ Mg	90.72	8.52	111.3	75	42.5
Gd- ²⁶ Mg	90.68	8.52	103.0	71	46.0
Gd- ²⁸ Mg	89.31	8.45	88.5	66	43.5
Gd- ²⁹ Mg	90.18	8.49	89.7	62	45.5

Curie temperatures were determined from Arrott (σ^2 versus χ^{-1}) plots (Fig. 3) at the temperature where spontaneous magnetization was first observed.

Although the alloys appear to order ferromagnetically, they do not saturate even at 1.4 T as shown in Fig. 4. The ferromagnetic moment increases as Gd concentration increases suggesting that Mg additions change the number of Gd-Gd nearest neighbors, and their separation has an effect on the $4f$ - $4f$ interactions via the conduction electrons [i.e., Ruderman-Kittel-Kasuya-Yosida (RKKY) interactions]. The maximum measured moment per Gd atom is only about $4.0\mu_B$, almost a factor of 2 lower than the $7\mu_B$ one would expect for Gd ions in a ferromagnetic state.

For comparison, a series of supersaturated α -Gd alloys were made by quenching from the α phase region near the eutectoid temperature. The Curie temperature decreases linearly with increasing Mg concentration as shown in Fig. 5. Extrapolation to pure Gd gives a value of 291 K, which compares quite well with accepted value for hcp Gd, 293 K,^{5,6} and gives us some confidence in the extrapolated value obtained for the hypothetical bcc Gd phase, which is 145 K, see Fig. 5. An extrapolation over such a wide composition range is tenuous. This is especially true in this case where there is likely to be a change in the type of ordering somewhere in the composition

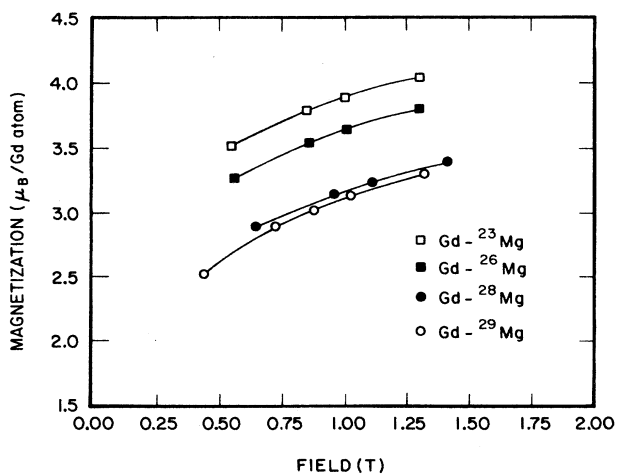


FIG. 4. Magnetization at 4.2 K vs applied field for some Gd-Mg alloys.

range (i.e., see below). Furthermore, in contrast to the bcc alloys, the hcp alloys are good ferromagnets with magnetization reaching $7\mu_B$. Whether these differences are due to the Mg diluent or crystal structure effects cannot be determined from these measurements.

The fact that the magnetic moments in the bcc Gd-Mg were so low made us suspicious that either antiferromagnetic ordering or some kind of spin-glass behavior was occurring. Evidence for a magnetic reentrant spin-glass transition can be seen from χ measured at low fields for the 28% alloy (Fig. 6). In these measurements the sample was zero-field cooled (ZFC) to 5 K, and χ was measured on heating with $B=0.005$ or 0.05 T. When 120 K was

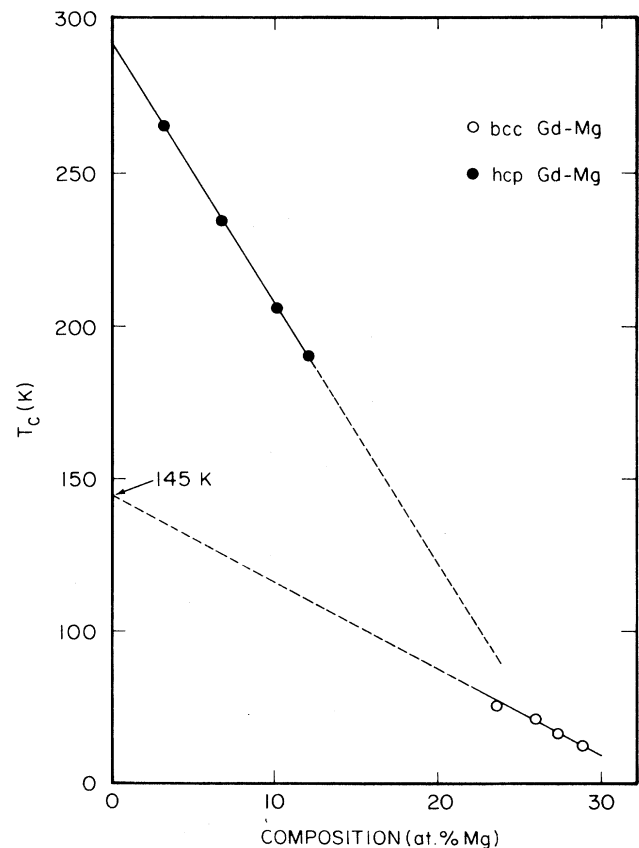


FIG. 5. Curie temperature vs composition for bcc and hcp Gd-Mg alloys.

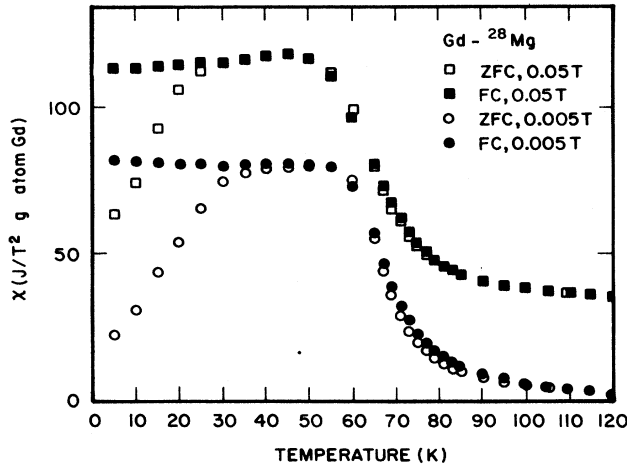


FIG. 6. Field-cooled (FC) and zero-field-cooled (ZFC) magnetic susceptibility for Gd- ^{28}Mg . The 0.05 T curves are offset by 35 units.

reached (~ 35 K above Θ_p) the sample was field cooled (FC), this time in the measuring field, and χ was measured on cooling. At low temperature, χ for the ZFC branch is dramatically lower than that of the FC branch.

This type of irreversibility is characteristic of spin-glass systems where the magnetic moments freeze in some random arrangement below a critical temperature T_f marked by the divergence of the FC and ZFC branches. In the ZFC branch this spin freezing process competes with the spontaneous magnetization due to the ferromagnetic alignment of spins below the Curie transition. However, if the sample is cooled in an external field as in the FC branch, the moments freeze in a preferred orientation (that of the ferromagnetic alignment) with no drop in χ at T_f .

The spin-glass state created by zero-field cooling can be destroyed by application of an external field and is observable by a reduction of T_f with increasing field. If T_f is taken as the divergent point of the FC and ZFC branches, one can see from Fig. 6 that T_f decreases from 50 to 35 K when B is increased from 0.005 to 0.05 T. The χ data for higher fields as in Fig. 2 were all ZFC measurements, and no downturn in χ exists showing that $B=0.8$ T is sufficient to completely revert the sample from the spin-glass state to the higher-field ordered state.

T_f was determined for each alloy by low-field (0.025 G) ac susceptibility as opposed to extrapolating low-field static χ data to zero field. χ_{ac} is shown for the four alloys in Fig. 7, all measured on heating. The 28% alloy was measured on both heating and cooling below the maximum with no difference in χ_{ac} . Normally T_f is marked by a sharp cusp in χ_{ac} , but for these alloys the high-temperature branch is lost due to the ferromagnetic transition. Lacking a cusp, T_f was defined as the intersection between a linear extrapolation of the low-temperature side of χ_{ac} with a horizontal line defined by χ_{ac} maximum. The results are plotted in a magnetic phase diagram along with the T_c 's in Fig. 8. The tendency is for

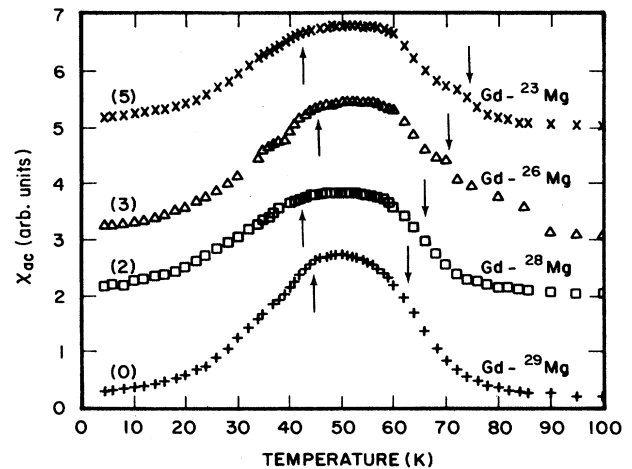


FIG. 7. ac magnetic susceptibility for Gd-Mg alloys. The number in parentheses is the amount of offset along the ordinate. The down arrows denote T_c 's from Arrott plots and the up arrows denote T_f .

T_f to increase with Mg composition, the reverse of the T_c dependence. Although a pure spin-glass behavior was never observed, it is predicted by Fig. 8 for alloys containing up to 66% Gd which would be an unparalleled large concentration of magnetic material for a metallic crystalline spin glass.

The heat capacity C has been measured for four bcc Gd-Mg alloys from 1.5 to 5 K. Each alloy was run several times consecutively with approximately 50 points per run such that for each alloy there are at least 200 data points. The large number of data points were taken to insure reproducibility and to enhance statistical fitting procedures. The strong curvature in the standard C/T versus T^2 plot (Fig. 9) is evidence of a large magnetic

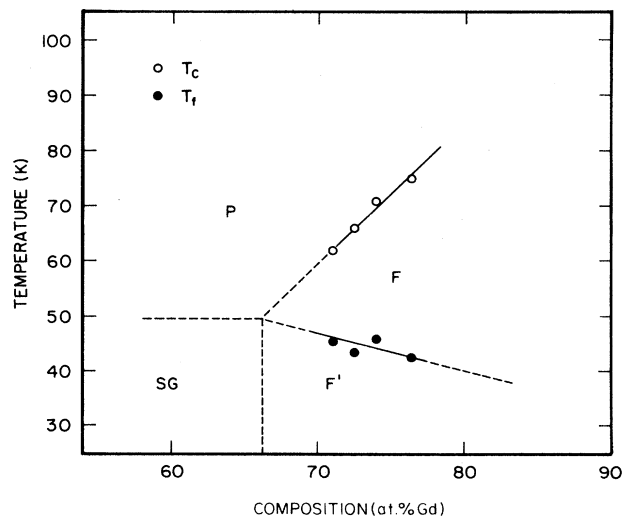
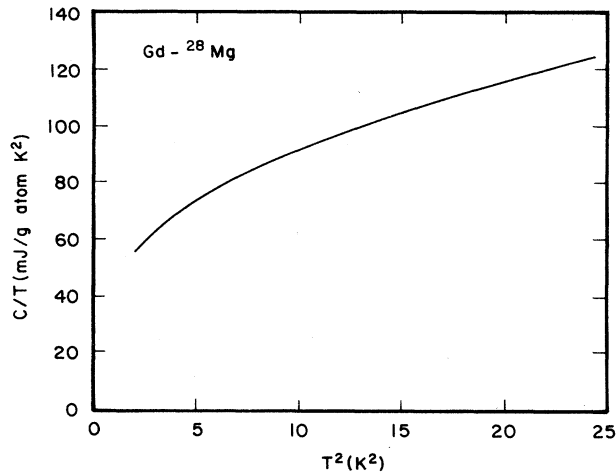


FIG. 8. Magnetic phase diagram for the Gd-Mg system where P, F, F', and SG are the paramagnetic, ferromagnetic, mixed ferromagnetic-spin-glass, and spin-glass phases, respectively.

FIG. 9. C/T vs T^2 for Gd-²⁸Mg.

term that overpowers the electronic and lattice terms. Even at the lowest temperatures (< 2 K) the curvature still persists preventing the normal extrapolation to obtain the electronic coefficient γ . The ordering temperatures for β -Gd were too high for our calorimeter to measure the heat capacity up to the magnetic transitions.

Reproducibility was only achieved if the sample was electropolished (6% perchloric acid in methanol at -60°C) just before cooling the sample in the cryostat. Similar behavior was reported for pure Gd by Hill *et al.*⁷ which was attributed to thin layers of ferromagnetic Gd_2O_3 on the surface that was removed by electropolishing.

At low temperatures the heat capacity of the β -Gd alloys can be represented as the sum of the electronic, lattice, and magnetic contributions (C_e , C_l , and C_m , respectively). The temperature dependence of C_e is linear, and C_l is a series of odd powers in T usually shortened to just T^3 for $T < \Theta_D/50$ where Θ_D is the Debye temperature.

The temperature dependence of C_m is complex in that from χ measurements both ferromagnetic and spin-glass excitations are expected. Assuming negligible anisotropy effects ($L=0$ and a cubic system) the ferromagnetic term can be written as DT^n where classically $n=1.5$. A linear dependence has been universally accepted for spin-glass systems, so the total heat capacity can be represented by

$$C = AT + BT^3 + DT^n, \quad (1)$$

where A , B , and D are constants and A would be the sum of the spin-glass contribution and the electronic specific-

TABLE II. Relative contribution (%) of the heat-capacity terms in the β -Gd model.

T (K)	C_e	C_l	C_m
1.50	14.0	1.4	84.6
1.75	13.0	1.7	85.4
2.00	11.9	2.1	86.0
2.25	11.1	2.5	86.4
2.50	10.5	2.9	86.6
2.75	10.0	3.3	86.8
3.00	9.5	3.7	86.8
3.50	8.6	4.6	86.8
4.00	7.9	5.6	86.5
4.50	7.4	6.5	86.1
5.00	6.9	7.5	85.6

heat coefficient γ . It has been well established that γ is not uniform across the lanthanide series,⁷⁻¹¹ so no estimate of γ was made.

A number of different fitting procedures were attempted with no success. An iterative graphical method¹¹ did not converge and brute-force statistical computer-fitting routines resulted in nonphysical parameters (e.g., $A < 0$) whether n was fixed at 1.5 or allowed to float.

The fitting method finally used was a two-step process. First, n was determined by assuming $C \approx K^n$. This assumption is valid because C_m comprises nearly 85% of the total heat capacity. In addition, trial and error modeling using Eq. (1) showed that as a percentage of C , C_m was remarkably constant from 2.25 and 4.00 K. The results of a calculation with $A=8$ mJ/g atom K^2 , $B=0.35$ mJ/g atom K^4 , $D=38$ mJ/g atom $\text{K}^{2.6}$, and $n=1.6$ is listed in Table II. Although the percentage of the total heat capacity for C_e and C_l decreases, and increases, with increasing temperature, respectively, the variations cancel each other out and C_m/C remains virtually constant. Second, these n 's were then used in Eq. (1) which was subsequently fit to the entire data of each alloy using a linear least-squares method. Table III summarizes the results. The error limits are the least-square standard deviations.

Table III shows that n is decreasing with decreasing Mg content as would be expected, because as the Mg content decreases the Curie temperature rises and this would tend to bring n closer to the classical value of 1.5. The relationship is not linear, but is approaching a value near 1.5. The Debye temperatures calculated from the B parameter show no clear composition dependence, but the values are reasonable [e.g., for pure hcp Gd (Ref. 7) $\Theta_D = 167$ K]. Because the contribution of C_l is small rel-

TABLE III. Summary of heat-capacity coefficients for β -Gd in mJ units.

Alloy	A	B	D	n	Θ_D (K)
Gd- ²³ Mg	8.06±0.39	0.37±0.02	37.5±0.3	1.620±0.002	174±4
Gd- ²⁶ Mg	7.02±0.33	0.33±0.02	39.3±0.2	1.651±0.002	181±4
Gd- ²⁸ Mg	6.79±0.48	0.37±0.02	38.1±0.3	1.656±0.002	173±5
Gd- ²⁹ Mg	4.79±0.44	0.27±0.02	35.5±0.3	1.688±0.003	193±5

ative to the magnetic and electronic contributions at these temperatures, Θ_D can only be known within 4 or 5 K. Taking this error into account, the Θ_D 's are nearly constant.

Values for A range from 4.79 to 8.06 mJ/g atom K² increasing with decreasing Mg content, however, a change of this magnitude cannot be explained by electron concentration effects. Leung *et al.*¹² predict γ for ferromagnetic bcc Gd to be as high as 11.4 mJ/g atom K², but with a slow decrease in γ with Mg composition within the limits of the rigid-band model. It seems likely, therefore, that the parameter A is a combination of γ and a spin-glass term.

B. β -Dy

As for Gd alloys χ for the β -Dy alloys was measured in fields up to 1.4 T (Fig. 10). The alloys follow Curie-Weiss behavior with Θ_p ranging from 31 to 35 K. A summary of the values are given in Table IV.

The type of magnetic ordering for the β -Dy alloys is different from that for the β -Gd alloys. Even though $\Theta_p > 0$, the alloys do not order ferromagnetically. Second, there is a maximum in the magnetization at ~ 15 K that persists up to magnetic fields of 1.4 T. Arrott plots as in Fig. 11 confirm no spontaneous magnetization down to 20 K where σ starts to decrease suggesting antiferromagnetic or spin-glass ordering. The magnetization maxima vary little with composition in contrast to the T_c 's of β -Gd which had a clear composition dependence, and the temperature of the maxima are independent of applied-field strength.

At low fields the maxima are better defined and less rounded. Figure 12 shows FC $\chi(T)$ for the 27% alloy. The leveling of χ below 15 K is typical of antiferromagnetic ordering for polycrystalline materials. If the sample is ZFC a large drop in χ is seen, but the maximum remains at the same temperature. There are two other features to be examined closely. First, the splitting of the FC and ZFC branches occurs *above* the ordering maximum which is unusual. If the field cooling irreversibili-

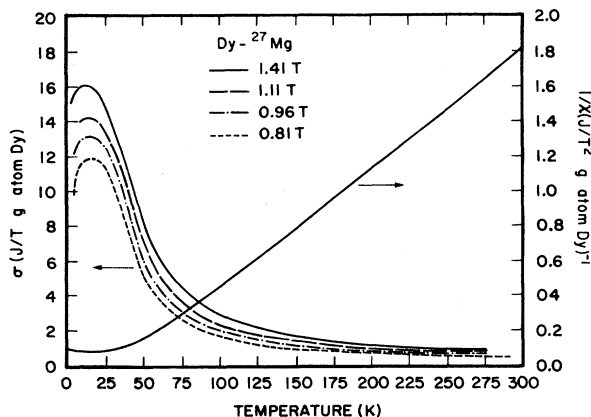


FIG. 10. Magnetization and inverse susceptibility for Dy-²⁷Mg, which is typical of all the Dy alloys.

TABLE IV. Summary of magnetic behavior in β -Dy.

Alloy	C	P_{eff} (μ_B)	θ_p (K)	T_f (K)
	$\left[\frac{\text{JK}}{T^2 \text{ g atom Dy}} \right]$			
Dy- ²⁷ Mg	149.10	10.92	31.4	30.0
Dy- ²⁸ Mg	147.36	10.86	35.1	31.0
Dy- ²⁹ Mg	145.91	10.80	31.6	30.5

ties are of spin-glass nature, one would expect that the spin-glass state would be favored at lower temperatures than an assumed antiferromagnetic state. Second, the leveling off in χ does not occur for the FC branch as it does for β -Gd alloys (Fig. 6). A nearly linear decrease in the ZFC χ down to 5 K is similar to the spin-glass transition in β -Gd. There seems to be both spin-glass and antiferromagnetic transitions going on with nearly the same ordering temperature. The splitting of the FC and ZFC curves above the cusp is more complex and may be the effect of competition between the two types of ordering. The maximum at 0.005 T (Fig. 12) is 10 K higher than that for the high-field measurements (Fig. 10), and as the field is increased to 0.2 T the maximum becomes more rounded and begins to shift to lower temperatures (Fig. 13).

The χ_{ac} (Fig. 14) for the three β -Dy alloys are nearly identical. A cusp in χ_{ac} is sharp and well defined and

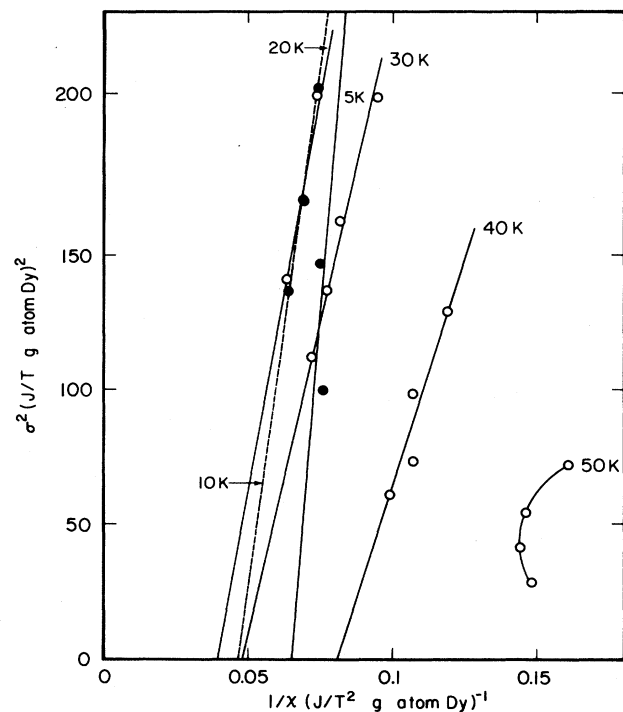


FIG. 11. Arrott plot for Dy-²⁷Mg. Note that there is no spontaneous magnetization. The solid circles and dashed line are for clarity.

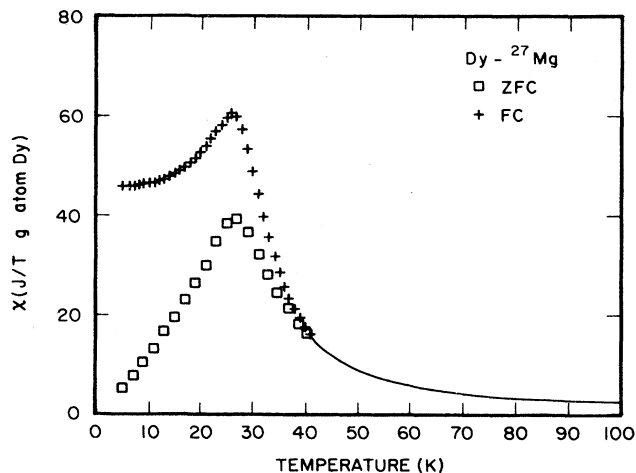


FIG. 12. Field-cooled (FC) and zero-field-cooled (ZFC) magnetic susceptibility for Dy-27Mg.

could represent spin-glass ordering. T_f , given by the maximum in χ_{ac} (Table IV), is the same within 1 K for all the compositions with the average of 30.5 K and does not show any obvious composition dependence.

The heat capacity up to 80 K has been measured for two of the alloys (Fig. 15). Above 60 K the scatter due to experimental limitations becomes too great for confident measurement. There is, however, a broad maximum between 40 and 50 K due to the magnetic ordering. The magnitude of the lattice contribution is increasing rapidly in this temperature range, and it should account for about 50% of the total heat capacity. Therefore, the actual maximum in C_m will be at a somewhat lower temperature.

For Dy there is also a hyperfine contribution C_h to the heat capacity so there are at least four terms contributing to the total heat capacity: electronic, lattice, hyperfine,

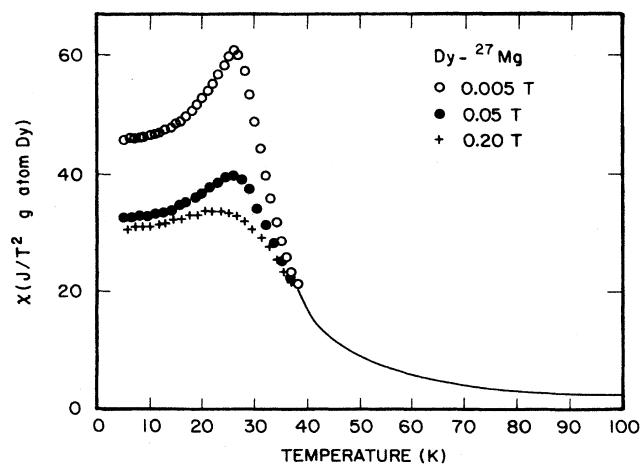


FIG. 13. Field-cooled magnetic susceptibility of Dy-²⁷Mg as a function of field.

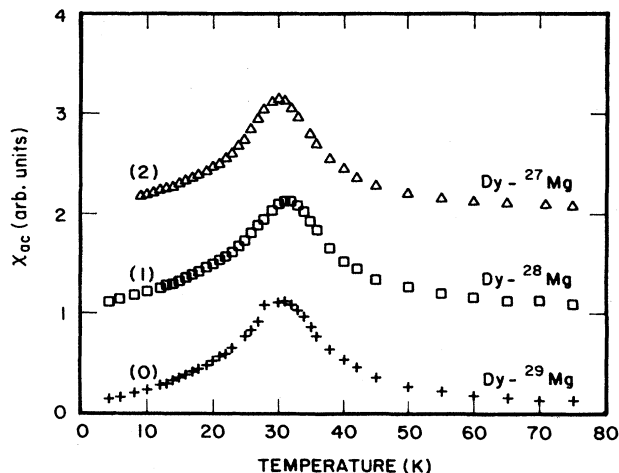


FIG. 14. ac magnetic susceptibility for three bcc Dy-Mg alloys. The offset along the ordinate is in parentheses. The cusp indicates T_f .

and magnetic. The hyperfine contribution arises from the two isotopes, Dy¹⁶¹ and Dy¹⁶³, both with nuclear spin $I = \frac{5}{2}$ giving six hyperfine levels each. Following the analysis of Hill¹³ for pure Dy, the high-temperature limit C_h can be represented above 1.6 K by

$$C_h = f(28.235T^{-2} - 1.6177T^{-3}) \quad (2)$$

for mJ/g atom K units, where f is the atomic fraction of Dy in the alloy.

Plots of $\ln(C)$ versus $\ln(T)$ predict a power law for C_m where $2 < n < 3$. However, the large linear region below 5 K as found for β -Gd are not observed for the Dy alloys, so a definite choice could not be made confidently. Thus two methods were tried.

Method I assumes a power-law dependence for C_m such that $C - C_h - C_l = AT + BT^n$ for $T < 5$ K. The lattice term will be dominated by the magnetic terms, so an estimate of C_l was subtracted from C in addition to C_h .

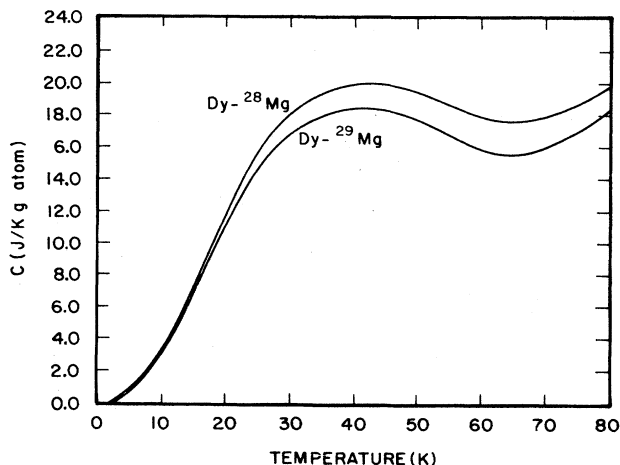


FIG. 15. Heat capacity vs temperature for two Dy-Mg alloys.

TABLE V. Summary of heat-capacity coefficients for β -Dy in mJ units.

	Alloy	A	B	D	Θ_D (K)
Method I	Dy- ²⁸ Mg	19.15	18.25	0.33 ^a	180 ^a
	Dy- ²⁹ Mg	17.64	16.42	0.33 ^a	180 ^a
Method II	Dy- ²⁸ Mg	15.34	20.92	1.35 ^b	
	Dy- ²⁹ Mg	12.72	19.77	1.11 ^b	

^aValue fixed before fitting.

^bIncludes both lattice and antiferromagnetic terms.

The value of Θ_D should not differ much between β -Gd and β -Dy, so the arbitrary value of 180 K was selected, a rough average of the Θ_D values for the β -Gd alloys (Table III). The 28 at. % alloy was reanalyzed for $\Theta_D = 170$ and 190 K. The change of Θ_D affected A and B by less than 2.5%, so the original choice of 180 K was retained. The best fit for both alloys occurs for $n = 2.2$; the corresponding values for A and B are given in Table V.

The values for A are different for both alloys and are much larger than to be expected for an electronic contribution alone. The presence of a linear heat-capacity term for spin glasses has been long known, and the excess linear term is attributed to spin-glass behavior. The $T^{2.2}$ term is empirical with no sound theoretical basis. However, some researchers have claimed a T^2 dependence in addition to the linear term for spin glasses.^{14,15} A plot of $(C - C_h - C_l)/T$ versus $T^{1.2}$ (Fig. 16) shows that the fit is good even up to 10 K.

Method II was based on the assumption that the alloys were in a mixed antiferromagnetic spin-glass state. The heat capacity corrected for the hyperfine contribution was fit to the form $AT + BT^2 + DT^3$ for $T < 5$ K. A contains both the electronic term and the linear spin-glass term, B would represent the spin-glass T^2 term, and D would represent C_l in addition to any antiferromagnetic excitations. The coefficients are also in Table V.

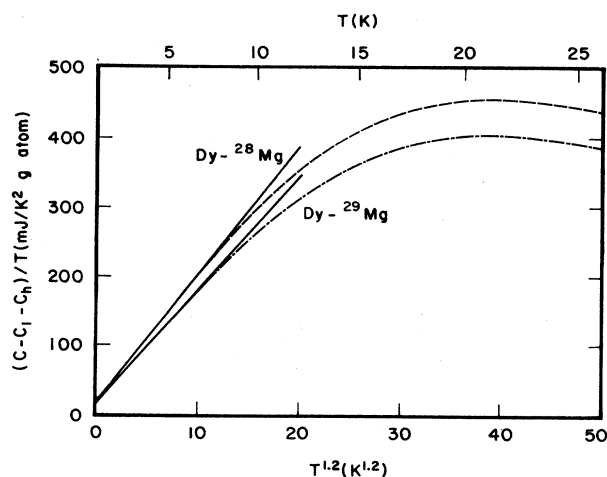


FIG. 16. $(C - C_l - C_h)/T$ vs $T^{1.2}$ for two Dy-Mg alloys. The straight lines are the least-squares fit of the data below 5 K.

The T^3 term is three to four times what would be expected for $\Theta_D = 180$ K ($D = 0.33$). The remaining part of the T^3 term would then be attributed to antiferromagnetism. The linear term is 25% to 30% lower than in the first method, but it is still too large to be attributable entirely to the electronic heat capacity. The large coefficient of the T^2 term (B) is indicative of its significance and favors the spin-glass hypothesis.

IV. DISCUSSION

A. β -Gd

The β -Gd alloys show evidence of reentrant spin-glass behavior. Some type of ferromagnetic ordering is present as illustrated by the Arrott plots (Fig. 3). The field cooling effects (Fig. 6) are typical of spin glasses. The loss of spontaneous magnetization in χ_{ac} curves is similar to that observed by Maletta and Felsch¹⁶ for $\text{Eu}_{0.5}\text{Sr}_{0.5}\text{S}$ and Manheimer *et al.*¹⁷ for $(\text{Fe}_x\text{Mn}_{1-x})_{75}\text{P}_{16}\text{B}_6\text{Al}_3$ where the transition from ferromagnetism to spin glass is well established by other means as well. Although the magnetic susceptibility shows spin-glass features, in themselves they are not conclusive.

The Gd-Mg system appears to have the right ingredients for spin frustration caused by competing exchange interactions. Ferromagnetic exchange interactions should dominate the system as apparent by the appearance of spontaneous magnetization and a large positive Θ_p . However, some antiferromagnetic interactions are likely to exist in light of the low spontaneous moment measured in high field and the lack of saturation.

The compound GdMg, CsCl structure, has been studied by two different groups both reporting unusual behavior. GdZn and GdCd are both good ferromagnets with T_c (268 and 270 K, respectively) just below that of pure Gd (293 K) and easily reach saturation ($\sim 7\mu_B$). GdMg, which has the same structure and electron concentration, has a much lower T_c (121 K) and is difficult to saturate,^{18,19} only reaching values of $6\mu_B$ which suggests that some antiferromagnetic ordering may occur in GdMg. Neutron diffraction cannot be made on Gd alloys due to high neutron absorption, but neutron diffraction has been done on TbMg (Refs. 18 and 20) which is similar to GdMg though with a lower Θ_p . These results indicate a structure of ferromagnetic sheets that are coupled antiferromagnetically producing a noncolinear ferromagnet. Of importance to this discussion is that the type of antiferromagnetic coupling could not be uniquely determined

with the investigators suggesting two or three equal alignments, an important ingredient for spin-glass formation. Aleonard *et al.*²¹ found the same type of structure in the RMg compounds with $R = \text{Dy}$, Ho , and Er as well.

Buschow and Oppelt¹⁹ discussed the possibility of disorder in GdMg structure, i.e., some Mg and Gd atoms interchange positions causing a disruption in the magnetic interactions. They claim a RKKY calculation shows a gradual change in Θ_p from a strong positive value for perfect ordering to negative values for complete disorder illustrating a mechanism to produce antiferromagnetic ordering. Buschow *et al.*²² later ruled out this possibility by neutron diffraction on NdMg, but the argument is appropriate for the β -Gd alloys of this study. A disordered CsCl structure is essentially a random bcc solid solution which is the same as β -Gd except that β -Gd has a lower concentration of Mg. This means that some intermediate Θ_p should be expected which decreases with increasing Mg concentration. This behavior is confirmed from χ^{-1} plots (Fig. 2 and Table I).

Buschow and Schinkel²³ decided that the antiferromagnetic interaction in GdMg is more fundamental in nature by studying the pseudobinary $(\text{Gd}_{1-x}\text{La}_x)\text{Mg}$. Just a 10% dilution of Gd by La induces a change from ferromagnetic ordering to antiferromagnetic ordering, so they asserted that a small antiferromagnetic interaction must be pre-existing in GdMg. A study of $\text{Gd}(\text{Mg}_x\text{Zn}_{1-x})$ (Ref. 19) shows that T_c increases with increasing Zn concentration or with decreasing lattice parameter. The same phenomenon is observed in the $(\text{Gd}_{1-x}\text{La}_x)\text{Mg}$ system indicating that the strength of the antiferromagnetic interaction depends on the interatomic distance as might be expected for RKKY interactions. There is evidence that the RKKY coupling in the lanthanide CsCl structure is carried in large part by $5d$ electrons.²⁴ Because this band is narrow, one would expect that the interaction would be sensitive to atomic spacing.

The distinction between the ordered CsCl structure and the random bcc structure is as follows. In the CsCl structure the Gd nearest neighbor is always a Mg ion and the second nearest neighbor is always another Gd ion. This gives rise to the ferromagnetic sheet structure in the RMg compounds. The antiferromagnetic interaction is between sheets, i.e., at longer range. In a random bcc solution, the nearest neighbor can be either a Mg ion or a Gd ion. The second nearest neighbor can also be either Mg or Gd. This uncertainty will disrupt the formation of the sheets with the finite probability that locally one ion may couple ferromagnetically and the next ion may order antiferromagnetically. If the interactions of all the atoms are considered then it is conceivable that the antiferromagnetic and ferromagnetic states may be equivalent for certain ions, but probably not for all depending of course on the environment surrounding the Gd ion in question. This competing interaction gives rise to the spin-glass-like behavior in the β -Gd alloys.

This picture favors a Gabay-Toulouse type²⁵ where a ferromagnetic phase transforms into a mixed F' state on cooling. A collinear ferromagnetic structure remains partially intact, but some of the spins freeze out of the

ferromagnetic alignments because of the competition between antiferromagnetic and ferromagnetic orderings.

Two transitions are measured with χ and χ_{ac} measurements indicating that such a disordering transition is present. T_f decreases with applied field showing that a field can overcome the spin frustration and force some kind of periodic order. The lack of saturation in the ferromagnetic state can be explained by the fact that with the removal of spin frustration there will still be a strong tendency for antiferromagnetic coupling as in the Mg compounds, and it requires much stronger fields to spin flip the $4f$ electrons into the ferromagnetic alignment.

The mixed F' state at low temperature is also supported by the heat-capacity data. The strong magnetic term is evidence of a remaining magnetic order. The temperature dependence which goes from $T^{1.6}$ to $T^{1.7}$ as Mg increases is reminiscent of a $T^{1.5}$ dependence for ferromagnetic magnon excitations. As the Mg concentration is decreased, the antiferromagnetic interactions lessen and one would expect the material to become more like a true ferromagnet ($T_f \rightarrow 0$) with n approaching 1.5 (see Table III). Increasing the Mg concentration should make β -Gd more spin-glass-like (higher T_f). A higher-order term of approximately T^2 has been established for CuMn (Ref. 14) and PtMn (Ref. 15) spin glasses, but in the case of β -Gd, spin-glass excitations interact with the ferromagnetic excitations giving an intermediate result but tending toward T^2 as the Mg concentration increases.

The existence of the linear term in C can also be explained by a F' state. In a simple model the linear coefficient at a given composition can be divided into three terms,

$$A = \gamma + \lambda\gamma + \eta, \quad (3)$$

where λ is a ferromagnetic enhancement factor and η is the spin-glass term. γ is proportional to the density of states at the Fermi level, and, therefore, it is sensitive to changes in band structure. γ can be considered a base electronic contribution combining both the ferromagnetic phase and the spin-glass phase, and would also include the usual enhancements that would affect both types of ordering equally such as electron-phonon coupling. If a rigid band structure is assumed over the concentration range, then there will be an electron concentration effect that will decrease γ as Mg concentration increases, but this effect is small.

In a ferromagnet there is often an enhancement λ of the electronic term due to spin waves. For pure Gd, this value may be as high as 1.⁹ This enhancement will depend on the Mg concentration in two ways. First, as the amount of ferromagnetic phase decreases (Mg increasing), there will be a decrease in λ proportional to the amount of ferromagnetic phase lost. Second, as the amount of ferromagnetic alignment decreases, the interactions necessary for electronic enhancement will be disrupted causing a further decrease in λ . These two effects will be additive leading to a strong negative dependence of A with increasing Mg content.

Finally there is the spin-glass term η . Since the alloys become more spin-glass-like at increased Mg concentration, one would expect η to increase with Mg concentra-

tion. But since the observed value of A drops rapidly with increasing Mg content η must be small as the negative dependence of the first two terms dominate. If the solid solution could be extended to higher Mg concentrations, then a leveling or an upturn in A might be observed as λ goes to zero. In conclusion, the above analysis of the concentration dependence of A indicates that the dominant term is $\lambda\gamma$.

B. β -Dy

Much of the same arguments used for β -Gd can be applied to β -Dy. DyMg has a weak net positive interaction ($\Theta_p = 25$ K), and it orders antiferromagnetically. The Θ_p 's for the β -Dy alloys are on the order of 30 K indicating a slight increase of the ferromagnetic exchange interaction by randomizing the bcc lattice.

This seems to be the opposite effect of the Gd-Mg system, but it is the same. In both DyMg and GdMg, the ordering is a system of ferromagnetic sheets with the antiferromagnetic coupling of the sheets larger in DyMg than for GdMg. In the GdMg system, a randomized lattice disrupting the ferromagnetic coupling and introducing antiferromagnetic exchanges explains the observed spin-glass ordering. The spin-glass behavior observed in the Dy-Mg system can also be explained by a randomization of the lattice, but in this case the antiferromagnetic ordering would be disrupted and stronger ferromagnetic exchanges would be introduced. Increasing the average ferromagnetic exchange relative to the average antiferromagnetic exchange interactions would introduce increased competition, and β -Dy would become a spin-glass candidate.

The ac magnetic susceptibility measurements show sharp cusps for all the compositions. The cusp, however, could be indicative of either spin-glass behavior or antiferromagnetism although the cusps are quite sharp, whereas antiferromagnetic cusps tend to be broader. Classical antiferromagnets usually show a leveling at some intermediate χ value especially for polycrystalline samples corresponding to a mixture of the parallel and perpendicular susceptibilities. But at zero field this magnetization may be small. By themselves, the χ_{ac} measurements are not conclusive.

High-field measurements show no spontaneous magnetization ruling out any sort of ferromagnetic phase. The χ curves at these fields show a maximum even at 1.5 T, a field that would normally destroy a spin-glass structure. This property favors antiferromagnetism.

For intermediate fields, a spin-glass-like irreversibility is observed between field cooling and zero-field cooling in the 27% alloy (Fig. 12). In a classical spin glass the onset of the irreversibility occurs at the maximum, but in this case the splitting of the FC and ZFC branches occurs at a temperature above that of the maximum. The FC branch for this alloy reaches a much higher value, but the maximum remains at the same temperature. In addition, the field-cooled branch now looks like a classical curve for an antiferromagnet. The coexistence of antiferromagnetism and spin-glass behavior has been confirmed²⁶ for $\text{Fe}_{1-x}\text{Mg}_x\text{Cl}_2$ but the split in this material is below a well

defined Néel temperature.

Baberschke *et al.*²⁷ have measured χ for ScDy and ScTb alloys containing about 5% Dy (Tb) and they report a similar splitting between ZFC and FC branches at temperatures higher than the χ maxima. An extensive study of the field dependence was also done where the maxima remained constant up to 0.06 T before shifting to lower T similar to the results in this study. The field study also allowed them to interpret their results as a resolution of the Almeida-Thouless²⁸ and Gabay-Toulouse²⁵ type transitions with the splitting being the Gabay-Toulouse²⁵ transition. This explanation fits the current data as well except for the extreme increase in χ for the FC branch. It is likely that there is a large antiferromagnetic component along with the spin-glass ordering and that both order at approximately the same temperature. The application of a small field may be just enough to make the antiferromagnetic state preferred for some of the Dy atoms.

The heat capacity is more revealing. At T_f there is a broad maximum in C_m like that of classical spin glasses. The sharp cusp that would be associated with antiferromagnetic ordering is not present implicitly, but could be covered up by a larger spin-glass heat capacity. The position of the heat-capacity maximum is not clear (Fig. 15), but it is within the accepted limits relative to the magnetic cusp (Fig. 13). The exact position of the maximum depends on the lattice correction and the amount and nature of any antiferromagnetic ordering in addition to the spin-glass ordering.

The low- T heat capacity gives the same information whether the first or second analysis discussed earlier (Sec. III B) is actually correct. The linear term is large and cannot be attributed to the electronic coefficient alone. Recently Hill and Gschneidner⁸ have accurately measured $\gamma = 4.9$ mJ for pure Dy. Even allowing a factor of 2 will not account for the large linear term of β -Dy. The largest portion of the linear term must therefore be due to spin-glass excitations.

Both analyses give a significant T^2 term which is indicative of spin glasses. If no T^3 term is included a $T^{2.2}$ term is required to give an adequate fit. This term would then be a combination of the T^2 spin-glass excitation and T^3 antiferromagnetic excitations. If a T^3 term is included a significant antiferromagnetic contribution is indicated, and the same conclusion is reached: a combination of antiferromagnetism and spin-glass behavior is present.

C. Atomic short-range order

We have mentioned above that the Mg-stabilized alloys are probably not perfectly random due to the dendritic freezing from the liquid. A second source of atomic short-range order may arise during the latter part of the quench. As an alloy is cooled through the eutectoid temperature there will be a driving force for the nucleation of α Gd (Dy) and GdMg (DyMg) which would require clustering of Mg atoms in some regions while depleting the Mg atoms in others. Even though the quench retains a "single phase" structure, the actual picture may be a collection of bcc atomic domains with varying Mg concentration.

Each domain may react magnetically different depending on the degree of clustering. The difference in magnetic properties from domain to domain will be further increased by the high symmetry of the bcc crystal which allows many favorable directions for atomic ordering. The aggregate collection of these domains will determine the macroscopic magnetic properties.

The importance of atomic short-range order is recognized²⁹ for classical spin-glass systems such as CuMn . It is a major reason for the formation of a spin glass as opposed to an Overhauser-type spin-density wave.³⁰ With respect to the bcc rare-earth alloys, atomic short-range order may be one mechanism to account for the mixed spin-glass behavior at such high concentrations. To explain further, some atomic domains may order (perhaps those at higher Mg concentrations) in a true spin-glass state while others may order ferromagnetically or antiferromagnetically. None of the ordering types can dominate on a long-range scale giving a mixed magnetic state.

V. CONCLUSIONS

It has been demonstrated that the metastable bcc $R\text{-Mg}$ alloys, $\beta\text{-Gd}$ and $\beta\text{-Dy}$, exhibit mixed spin-glass order. A pure spin-glass phase should not be expected because of the high content of magnetic material in the alloys that increase the probability of normal modes of magnetic coupling. In the case of $\beta\text{-Gd}$, strong ferromagnetic exchange interactions dominate, but there is a

Gabay-Toulouse type of transition from the ferromagnetic phase to a mixed ferromagnetic-spin-glass phase. In contrast, the $\beta\text{-Dy}$ alloys feature stronger antiferromagnetic interactions, and only one transition appears to occur from the paramagnetic state to a mixed antiferromagnetic-spin-glass state.

These spin-glass alloys are unusual in that they contain 70–75 at. % magnetic lanthanide atoms. Other spin-glass systems have been reported with high concentrations of magnetic material, e.g., insulating $(\text{EuSr})\text{S}$ and $(\text{FeMg})\text{Cl}_2$ or amorphous $\text{Gd}_{0.37}\text{Al}_{0.63}$, GdCu , and $(\text{FeMn})_{75}\text{P}_{16}\text{B}_6\text{Al}_3$.^{16,17,26,31–34} The Gd-Mg and Dy-Mg alloys of this study are unique in that they are both *crystalline* and *metallic*, and, to our knowledge, these alloys have the highest concentration by far of magnetic atoms of any *similar* material exhibiting spin-glass behaviors.

ACKNOWLEDGMENTS

The authors would like to thank Mr. J. Ostenson and Mr. W. Lee for help with the magnetic measurements and Mr. J. Moorman for technical assistance. This material is based on work supported by the National Science Foundation (J.W.H.) and by Ames Laboratory, operated for the U.S. Department of Energy by Iowa State University under Contract No. W-7405-ENG-82. This work was supported by the Office of Basic Energy Sciences.

*Present address: Magnequench, Delco Remy, 6435 S. Scatterfield Road, Anderson, IN 46013.

¹A. E. Miller and A. H. Daane, *Trans. Met. Soc. AIME* **230**, 568 (1964).

²J. W. Herchenroeder and K. A. Gschneidner, Jr., *Bull. Alloy Phase Diag.* **9**, 2 (1988).

³J. W. Herchenroeder, P. Manfrinetti, and K. A. Gschneidner, Jr., *Physica B* **135**, 445 (1985).

⁴P. Manfrinetti and K. A. Gschneidner, Jr., *J. Less-Common Met.* **123**, 267 (1986).

⁵S. Legvold, in *Ferromagnetic Materials*, edited by E. P. Wohlfarth (North-Holland, Amsterdam, 1980), Vol. 1, p. 183.

⁶K. A. Mc Ewen, in *Handbook on the Physics and Chemistry of Rare Earths*, edited by K. A. Gschneidner, Jr. and L. Eyring (North-Holland, Amsterdam, 1978), Vol. 1, p. 411.

⁷R. W. Hill, S. J. Collocott, K. A. Gschneidner, Jr., and F. A. Schmidt, *J. Phys. F* **17**, 1867 (1987).

⁸R. W. Hill and K. A. Gschneidner, Jr., *J. Phys. F* **18**, 2545 (1988).

⁹T.-W. E. Tsang, K. A. Gschneidner, Jr., F. A. Schmidt, and D. K. Thome, *Phys. Rev. B* **31**, 235 (1985).

¹⁰K. Ikeda, K. A. Gschneidner, Jr., T. Takeshita, D. W. Jones, and S. P. Farrant, *Phys. Rev. B* **31**, 5878 (1985).

¹¹J. A. Morrison and D. M. T. Newsham, *J. Phys. C* **1**, 370 (1968).

¹²T. C. Leung, X. W. Wang, and B. N. Harmon, *Physica B* **149**, 131 (1988).

¹³R. W. Hill (private communication).

¹⁴W. E. Fogle, J. D. Boyer, R. A. Fisher, and N. E. Phillips, *Phys. Rev. Lett.* **50**, 1815 (1983).

¹⁵T. Sato and Y. Miyako, *J. Phys. Soc. Jpn.* **51**, 2143 (1982).

¹⁶H. Maletta and W. Felsch, *Z. Phys. B* **37**, 55 (1980).

¹⁷M. A. Manheimer, S. M. Bhagat, and H. S. Chen, *J. Magn. Mater.* **38**, 147 (1983).

¹⁸R. Aleonard, P. Morin, J. Pierre, and D. Schmitt, *Solid State Commun.* **17**, 599 (1975).

¹⁹K. H. J. Buschow and A. Oppelt, *J. Phys. F* **4**, 1246 (1974).

²⁰G. Will, W. Schafer, and K. H. J. Buschow, in *Proceedings of the 12th Rare Earth Research Conference*, edited by C. E. Lundin (University of Denver, Denver, CO, 1976), Vol. 1, p. 41.

²¹R. Aleonard, P. Morin, J. Pierre, and D. Schmitt, *J. Phys. F* **6**, 1361 (1976).

²²K. H. J. Buschow, B. van Laar, and J. B. A. A. Elemans, *J. Phys. F* **4**, 1517 (1974).

²³K. H. J. Buschow and C. J. Schnikel, *Solid State Commun.* **18**, 609 (1976).

²⁴G. Weimann, H. Bopp, B. Elschner, and K. H. J. Bushow, *Int. J. Mag.* **5**, 1 (1973).

²⁵M. Gabay and G. Toulouse, *Phys. Rev. Lett.* **47**, 201 (1981).

²⁶P.-Z. Wong, S. von Molnar, T. T. M. Palstra, J. A. Mydosh, H. Yoshizawa, S. M. Shapiro, and A. Ito, *Phys. Rev. Lett.* **55**, 2043 (1985).

²⁷K. Baberschke, P. Pureur, A. Fert, R. Wendler, and S. Senoussi, *Phys. Rev. B* **29**, 4999 (1984).

²⁸J. R. L. de Almeida and D. J. Thouless, *J. Phys. A* **11**, 983 (1978).

²⁹A. F. J. Morgownik and J. A. Mydosh, *Solid State Commun.* **47**, 325 (1983).

³⁰J. A. Mydosh, *J. Appl. Phys.* **63**, 1 (1988).

- ³¹D. Bertrand, F. Bensamka, A. R. Fert, J. Gelard, J. P. Redoules, and S. Legrand, *J. Phys. C* **17**, 1725 (1984).
- ³²T. R. McGuire, T. Mizoguchi, R. J. Gambino, and S. Kirkpartick, *J. Appl. Phys.* **49**, 1689 (1978).
- ³³C. R. Fincher, S. M. Shapiro, A. H. Palumbo, and R. D. Parks, *Phys. Rev. Lett.* **45**, 474 (1980).
- ³⁴Y. Yeshurun, M. B. Salamon, K. V. Rao, and H. S. Chen, *Phys. Rev. Lett.* **45**, 1366 (1980).